REPORT DOCUMENTATION PAGE

Form Approved
OMB No. 0704-0188

1. REPORT DATE *(DD-MM-YYYY)*	2. REPORT TYPE	3. DATES COVERED *(From - To)*
	Technical Paper	

4. TITLE AND SUBTITLE

5a. CONTRACT NUMBER

5b. GRANT NUMBER

5c. PROGRAM ELEMENT NUMBER
62500F

6. AUTHOR(S)

5d. PROJECT NUMBER
2308

5e. TASK NUMBER
M4S7

5f. WORK UNIT NUMBER
345382

7. PERFORMING ORGANIZATION NAME(S) AND ADDRESS(ES)

8. PERFORMING ORGANIZATION REPORT

9. SPONSORING / MONITORING AGENCY NAME(S) AND ADDRESS(ES)

Air Force Research Laboratory (AFMC)
AFRL/PRS
5 Pollux Drive.
Edwards AFB CA 93524-7048

10. SPONSOR/MONITOR'S ACRONYM(S)

11. SPONSOR/MONITOR'S NUMBER(S)

12. DISTRIBUTION / AVAILABILITY STATEMENT

Approved for public release; distribution unlimited.

13. SUPPLEMENTARY NOTES

See attached 13 papers, all with the information on this page.

14. ABSTRACT

15. SUBJECT TERMS

16. SECURITY CLASSIFICATION OF:			17. LIMITATION OF ABSTRACT	18. NUMBER OF PAGES	19a. NAME OF RESPONSIBLE PERSON
a. REPORT	b. ABSTRACT	c. THIS PAGE			Kenette Gfeller
Unclassified	Unclassified	Unclassified	A		19b. TELEPHONE NUMBER *(include area code)* (661) 275-5016

AIAA 96-2730

Life Extension Strategies for Space Shuttle-Deployed Small Satellites Using a Pulsed Plasma Thruster

D.L. Tilley and R.A. Spores
Phillips Laboratory
Edwards AFB, CA 93524

32nd AIAA/ASME/SAE/ASEE
Joint Propulsion Conference
July 1-3, 1996 / Lake Buena Vista, FL

Life Extension Strategies for Space Shuttle-Deployed Small Satellites Using a Pulsed Plasma Thruster

Dennis L. Tilley*, Ronald A. Spores†
Phillips Laboratory
Edwards AFB, CA 93524

Abstract

At typical Space Shuttle altitudes atmospheric drag is the dominant force limiting satellite on-orbit life (typically < 100 days). The pulsed plasma thruster (PPT) is ideally suited to extend the life of small satellites deployed from the Shuttle due to its low system mass and volume, high specific impulse, and inert solid propellant (Teflon). The objective of this study was to identify and analyze life extension strategies for Space Shuttle-deployed small satellites using the pulsed plasma thruster. A generalized analysis is presented which is applicable to a broad range of satellite, PPT performance and life characteristics. Many PPT thrusting strategies were identified, enough to fit most spacecraft operational scenarios, for significantly extending small satellite on-orbit life. Within the limits of typical small satellite power to mass ratios, the most capable of these strategies, designated Lift & Coast, requires the least amount of propellant and is capable of extending life to 1-2 years with state-of-the-art PPT technology. In addition, within the context of PPT operation, preferential launch windows and strategies for reducing satellite drag were also discussed.

I. Introduction

Life extension strategies for Space Shuttle-deployed small satellites using a pulsed plasma thruster (PPT) are presented and analyzed. At typical Space Shuttle altitudes (140-240 nm) atmospheric drag is the dominant force limiting satellite on-orbit life. Depending on solar activity, typical orbital lifetimes are less than 100 days, which is too short to be useful for many missions. A detailed analysis of the life extension capabilities is required since the PPT thrust and drag force are comparable. The analysis is further compounded by the significance of variations in the thermosphere. Previous work investigating the use of PPTs for small satellite drag compensation are very sparse and illustrative in nature[1,2]; in fact, the application of propulsion systems (including electric) to small satellite missions has only recently received increased attention[2-6]. This analysis is an extension of previous work, and should also apply to small satellite deployment from the Space Station and MIR. Also discussed in this paper is the impact of the strategies on spacecraft power requirements and flight operations.

The primary motivation for this study was to identify PPT thrusting strategies which most efficiently extend the life of small satellites deployed from the Space Shuttle Hitchhiker Eject System (HES)[7]. Due to its inert nature, especially when unpowered, the PPT is well suited for Shuttle-deployed satellites because of minimal safety-related test and documentation requirements. Furthermore, since the HES provides reliable and inexpensive access to space, there is currently considerable interest in the small satellite community in utilizing it for satellite deployment.

The Phillip's Laboratory's MightySat Program has identified the Space Shuttle as a possible launcher for its small satellites[8]. Recently, elements of this analysis were used to investigate the extension of MightySat Flight II.1 to greater than one year using a PPT. In addition, a joint Phillips Laboratory/NASA LeRC/Olin Aerospace Company/Jet Propulsion Laboratory program has been established to demonstrate PPT life-extension capability on the MightySat II.1 flight. A second motivation for this work was to provide PPT design guidelines for this application, specifically for the PPT system to be flown on the MightySat II.1 flight.

The PPT is an electric propulsion device which uses electrical power to ionize and electromagnetically accelerate a plasma to high exhaust velocities (10-20 km/sec)[9-20]. Its high specific impulse enables significant reduction in propellant mass requirements compared to monopropellant and cold gas systems. A schematic of the PPT is shown in figure 1. It essentially consists of a bar of teflon, which is the propellant source, pressed firmly between two electrodes by a negator spring (which is the only moving part). A power processing unit (PPU) charges a capacitor to voltages in the 1000-2000V range using unregulated power from the spacecraft bus. The PPU also supplies a high voltage pulse to a spark plug which is used to ignite the discharge. Once the discharge is ignited, the energy stored in the capacitor (~20-40 J) powers a high current/low duration plasma discharge (~20 kA, ~5-10 μs) which ablates a small amount of teflon from the face of the propellant bar and electromagnetically accelerates it to high exhaust velocities. As it is consumed, propellant is continually replenished by the negator spring. The pulsed operation of the PPT allows it to operate over an extremely wide range of power levels at the same performance level. Average spacecraft bus power supplied to the PPT is dictated by the pulse rate (typically on the order of 1 Hz).

The PPT is ideally suited to the propulsion needs of small satellites because it is compact, uses an inert solid

* Research Engineer, Electric Propulsion Lab, Member AIAA

† Group Leader, Electric Propulsion [illegible] ber AIAA

propellant (Teflon), is easily integrated to a spacecraft, and has a low system wet mass (<5 kg). Due to its efficient fuel consumption and low power requirements (1-150 W), the PPT can significantly enhance small satellite maneuvering capabilities. Potential applications[2] include attitude control (including the complete replacement of a reaction wheel system), orbit maintenance/precision control, orbit raising/repositioning and deorbit. PPTs have flown on LES 6 [9-11], TIP II & III[12,13], NOVA I, II, III[14,15], as well as on Japanese[16] and Chinese[17] spacecraft. PPTs have also been flight qualified for the LES 8/9[18,19] and SMS spacecraft[20]. Although the above flight-qualified PPTs have performed flawlessly on several satellites, unfortunately for small satellite designers, these models are no longer available for purchase. In addition, the performance of previous flight-qualified models are not well suited for the more ambitious life extension missions discussed in this paper, especially for >100 kg satellites. The absence of an off-the-shelf flight qualified PPT has recently spurred PPT R&D programs at the Phillips Laboratory, NASA Lewis Research Center, Olin Aerospace Company, and others, with goals to significantly increase performance and decrease system wet mass, while maintaining as much as possible the flight heritage of previous designs.

This paper first presents a brief description of the advanced PPT flight demonstration on the MightySat spacecraft in section II. In section III, strategies for extending Shuttle-deployed small satellite life with the PPT are reviewed and analyzed. Conclusions are presented in section IV. Following the references section is a nomenclature section, and Appendix A where the analysis model is derived in detail.

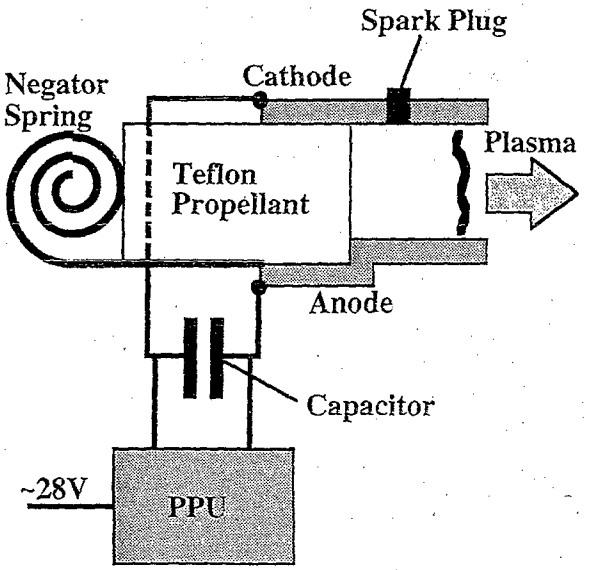

Fig. 1: The pulsed plasma thruster (PPT).

II. Advanced Pulsed Plasma Thruster Demonstration on MightySat Flight II.1

The Phillips Laboratory is currently leading a joint effort to demonstrate an advanced pulsed plasma thruster on the MightySat II.1 space flight (launch Jan 99)[21]. MightySat II.1 is a 250 lb.-class satellite to be manufactured by Spectrum Astro, Inc. of Gilbert, AZ under contract with the Space Experiments Directorate of the Phillips Laboratory at Kirtland A.F.B., NM. Although the launch vehicle is to be determined, the Space Shuttle HES is one option currently being examined. Participants in the joint PPT flight demonstration effort include the Phillips Laboratory (Propulsion Directorate), NASA Lewis Research Center, Jet Propulsion Laboratory, and Olin Aerospace Company. In addition to leading the flight program, the Phillips Laboratory is primarily responsible for PPT/spacecraft integration & test, flight operations, and flight data analysis. Olin Aerospace Company is developing the flight PPT, under a contract with the NASA Lewis Research Center. In addition to leading flight PPT development, the NASA-Lewis Research Center will also perform PPT plume compatibility ground tests and PPT plume modeling tasks. The Jet Propulsion Laboratory will provide two QCM/calorimeter pairs to serve as sensors to measure potential spacecraft surface deposition from the PPT exhaust plume, and will also support ground and flight sensor data analysis.

The PPT to be demonstrated on Flight II.1 will provide a dramatic leap in capability compared to previous flight-qualified models. Power handling capability will be as high as 150 W and the system wet mass goal is <3.5 kg for a 20,000 N-s total impulse[2]. As part of the flight demonstration, the advanced PPT will perform an orbit raising mission to significantly increase spacecraft orbital life. If MightySat II.1 is deployed from the Space Shuttle, the orbit raising maneuver will be critical for achieving an on-orbit life of one year.

Beyond the actual use of the PPT for Flight II.1 life extension, the objectives of the demonstration are twofold. First, demonstrate advanced PPT in-flight performance and life on a viable spacecraft. Second, demonstrate compatibility of the PPT with the spacecraft and optical sensor payloads. Potential compatibility issues include EMI, thermal loading, and contamination of optical surfaces. In addition, this demonstration will serve as a pathfinder for demonstrating PPT compatibility with Shuttle integration requirements. Spacecraft PDR and CDR are scheduled to be in October and December 1996, and PPT CDR is scheduled for September 1996. PPT integration and test will begin in November 1997.

III. Life Extension Strategies

Due in part to the MightySat mission, the focus of this study was to identify strategies to extend small satellite life to 1-2 years. The orbit raising model, thermospheric model, critical assumptions, and the numerical routine used in this analysis are discussed in detail in Appendix A. Assuming a circular orbit, there are essentially four

parameters which are required to define the trade space for this study: initial altitude, where the Shuttle first deploys the satellite; β, the orbit-averaged satellite ballistic coefficient; a, the orbit-averaged spacecraft acceleration due to PPT thrust alone; and $F_{10.7}$, the solar radiative flux at the earth's surface at 10.7 cm, which is commonly used as a proxy for solar activity in the ultraviolet spectrum.

A specified value of the PPT specific impulse is not required to perform the orbital analysis because the total propellant mass is assumed to be much smaller than the spacecraft dry mass, which is generally true for PPT systems. However, once the above four parameters and the thrusting duration are fixed, the specific impulse is required to determine the required propellant mass. Consistent with the above assumption, it is also assumed that the spacecraft mass and the orbit-averaged satellite ballistic coefficient do not change appreciably throughout the PPT thrusting duration. Solar array degradation and the time required for initial satellite on-orbit check-out and outgassing were not considered in this study.

In order to limit the trade space involved, typical ranges of the above four parameters are first reviewed. An initial altitude range of 140-240 nautical miles (nm) is typical of the Space Shuttle[22]. Although the Shuttle can reach altitudes lower and higher than this range, it is shown later that 140-240 nm is the region of practical interest in using the PPT for life extension.

An expression for the orbit-averaged satellite ballistic coefficient is shown in equation 1:

$$\beta = \frac{m}{t_p}\left[\int_0^{t_p} C_d(t)A(t)dt\right]^{-1} = \frac{m}{\overline{C_d A}} \qquad (1)$$

where m is the spacecraft mass, C_d is the drag coefficient, A is the satellite cross-sectional area, and t_p is the orbital period. A range of 10-50 kg/m^2 should span typical values of β for small and microsatellite designs to be deployed from the HES[23]. For the MightySat II case using an upgraded HES, m~125 kg, A~1.5 m^2, C_d~2, results in a β~40 kg/m^2.

Two extreme values of $F_{10.7}$ were assumed: one to represent solar minimum *plus* 2σ levels ($F_{10.7}$=80x10^{-22} Wm^{-2}Hz^{-1}), and the other to represent solar maximum conditions *plus* 2σ levels ($F_{10.7}$=240 x10^{-22} Wm^{-2}Hz^{-1})[24]. To compensate for the highly random nature of the thermosphere, 2σ levels were used because these are the minimum levels to which a typical spacecraft/PPT system would be designed. No effort was made to account for geomagnetic storms on PPT life extension performance; although, their effects are discussed later.

The parameter a is a measure of available power and PPT performance divided by the spacecraft mass. This parameter generalizes the analysis to make it applicable to a wide range of PPT performance and life, spacecraft mass, and flight operations. A common expression for a is shown in equation 2:

$$a = \frac{f_s\overline{T}_s + (1-f_s)\overline{T}_d}{m} \qquad (2)$$

where:

$$\overline{T} = \frac{2\eta P}{I_{sp}g} \qquad (3)$$

where f_s is the fraction of the orbit that the spacecraft solar arrays are illuminated by the sun, $\overline{T}_s$ is the time-averaged thrust of the PPT while the spacecraft is in sunlight, and $\overline{T}_d$ is the time-averaged PPT thrust while the spacecraft is in shadow. Equation 3 shows the explicit dependence of the average thrust on power input to the PPT, where η is the efficiency of the PPT system, accounting for inefficiencies in the power processing unit and in the thruster's capability to transform energy stored in the capacitor into useful thrust, P is the power input, I_{sp} is the specific impulse, and g is the gravitational acceleration at the earth's surface (= 9.81 m/s^2). Typical values of the above parameters for a state-of-the-art PPT are η =0.1 and I_{sp} =1000 sec.

The distinction of average thrust is required because the PPT is a pulsed device, where the average thrust is equal to the product of the impulse bit per shot and the pulse frequency. Average thrust has meaning and is useful when the time scale of the life extension maneuver is much longer than the inverse pulse frequency. This criteria is easily satisfied in this analysis where transfer times are ~10 days, and the inverse pulse frequency is ~100 msec.

The parameter f_s generally varies throughout a thrusting maneuver, and is a function of orbit inclination, altitude, the right ascension of the ascending node, and time of year. Due to the desire to limit the trade space involved, and because the variation of f_s can be well represented by an average value, a is assumed constant.

Using equation 2 and 3, typical PPT performance values (η =0.1, I_{sp} =1000 sec), and typical small satellite *payload* (not total) power to mass ratios (0.3-1.0 W/kg, reference 23), a range of a was chosen to be from 0.7 - 2.1 μg. The use of typical small satellite payload power to mass ratios is extremely useful for assessing the practicality of using the PPT for life extension. For instance, this range represents typical maximum values of a, where the entire payload power is devoted to PPT operation. While the payload is operational, considerably less power (probably no greater than 1/10th of full power) is available to use the PPT for orbit maintenance.

Before reviewing the various life extension strategies, it is useful to examine the orbital life of typical small satellites deployed from the Shuttle. Shown in figure 2 is a plot of satellite life for the above described parameters and with end-of-life defined as when the spacecraft falls below 130 nm. Depending on solar conditions and the satellite ballistic coefficient, orbital decay times range from as little as a few days to over three years. Note that for deployment above 215 nm, for β>30 kg/m^2 at solar minimum, a propulsion system is not required to extend satellite life to 1-2 years; although, the PPT is well suited to extend satellite life beyond 2 years.

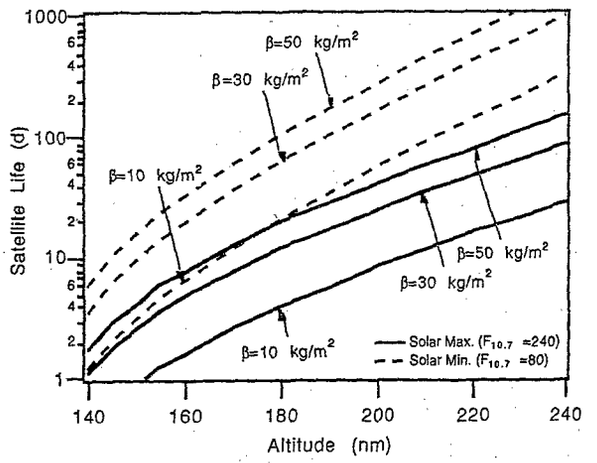

Figure 2: Characteristic small satellite on-orbit life (2σ worse case) when deployed from the Space Shuttle.

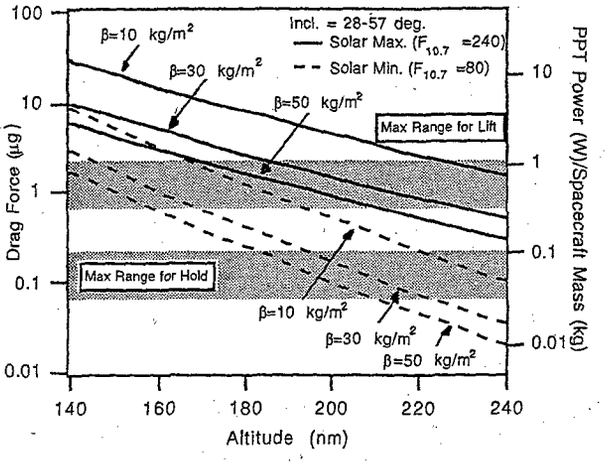

Figure 3: Drag force and PPT power required to maintain the orbit at typical Shuttle altitudes (2σ worse case).

III.1 Hold

The first life extension strategy to be investigated is to use the PPT, at the Shuttle-deployed altitude, to provide an orbit-averaged force which exactly compensates the drag force. This life extension strategy is designated *Hold*, as inspired by the use of this term in Zondervan, et al.[25]. This PPT operational scheme is not new, and is exactly that used on the NOVA satellites[14,15]. The NOVA satellites were operated at an altitude of 634 nm, where on-orbit life is not an issue (the PPT system was used for precise orbit maintenance, and was fired about once per minute).

Shown in figure 3 is the 2σ worse case drag force as a function of typical Shuttle altitudes and inclinations, the orbit-averaged ballistic coefficient, and the $F_{10.7}$ index. In this paper, the value of a required to negate the drag force at the *Shuttle-deployed altitude* is denoted as a^*. The parameter a^* is very important in this study, and will often dictate whether a particular strategy is feasible or not (see equation A15 in the Appendix). The right scale of figure 3 shows the orbit-averaged power divided by the total spacecraft mass (the specific power) required for a PPT with SOA performance (η=10%, I_{sp}=1000 sec) to perform the Hold mission. For example, at 1 W/kg, a 50 kg satellite requires 50 W of orbit-averaged power to maintain the satellite's altitude.

The Hold mission, by definition, requires the PPT and payload to operate concurrently on-average during each orbit. Assuming, at best, that 10-15% of the orbit-averaged payload power is available to the PPT, plus including a reasonable safety factor for reasons to be described later, leads to about 0.03 to 0.1 W/kg available for the PPT for the Hold mission (see the lower shaded region in figure 3). Based on this assumption, the Hold strategy requires too much power to be practical for most satellite designs, and will not work at solar maximum. Even at solar minimum, the Hold strategy is only practical at the highest Shuttle orbits where orbital life is already long. The propellant mass requirements are also high for the Hold strategy, as will be discussed in more detail in section III.3.

III.2 Lift & Coast

After the Shuttle deploys the satellite, an alternative life extension option is to use all of the power available to the payload to boost the satellite to a higher altitude. As shown in figure 2, satellite life after the transfer can be significantly enhanced using this strategy, which is designated Lift & Coast, where Lift is again an appellation used in Zondervan, et al.[25]. The obvious trade-off between this strategy and Hold, is the constraint of operating the payload on standby power during the transfer, which may have a duration of up to a few months.

With the payload operating in standby-mode, an upper limit of 0.3-1 W/kg is available for propulsion (see the upper shaded region in figure 3). The PPT is of limited use during solar maximum conditions at altitudes below 170 nm. At solar minimum, the PPT is of limited use at altitudes below 140 nm, and also for altitudes above 210 nm with β>30 kg/m² (where orbital decay times without propulsion are in the 1-2 year range).

Within the above PPT applicability limits, a large region of trade space is accessible for using the PPT to extend satellite life using the Lift & Coast strategy. Figures 4-8 illustrate the benefits of the Lift & Coast strategy, and span most of the trade space involved. Plotted is the satellite life *after* the PPT orbit raising maneuver versus the PPT thrusting duration. Each plot spans a range of a and initial altitude for a given level of solar activity and β. As the thrusting duration is reduced to zero, the satellite life is reduced to its natural orbital decay life at the given initial altitude and β. As expected, for a given transfer time, increasing the value of a significantly increases satellite life. Alternatively stated, providing more power for propulsion and increasing PPT efficiency is highly desirable to reduce the transfer time required to achieve long life.

Note that when thrust is much greater than the initial drag force (a>>a^*, where values of a^* are also shown in figures 4-8), transfer times of 10-30 days are typically required to achieve a 1-year life. When the thrust is only

slightly greater than the initial drag force ($a \sim a^*$), transfer times are typically much longer (>100 days). When the thrust is less than the initial drag force ($a<a^*$), satellite life (without PPT operation) actually reduces with thrusting duration. However, the total time in orbit (PPT thrusting time plus non-thrusting time) is in fact increased by using the PPT, since the PPT is reducing the rate of orbital decay. Although factors of 2-3x life extension can be obtained in this case, it is generally not possible to extend life to 1-2 years when $a<a^*$. In the remaining portion of the paper, comparisons will be made of strategy characteristics for two representative cases: $a>>a^*$ and $a \sim a^*$. The expression $a \sim a^*$ implies $a^*<a<\sim 1.5a^*$.

Increasing the power level significantly improves the life enhancement capability of the PPT. In fact, increasing the solar array area to provide more PPT power compensates quite well for the drag increase and the need to raise the satellite to a higher altitude to achieve a the same life (compare the β=30 kg/m^2, a=0.7 μg case to the β =10 kg/m^2, a=2.1 μg case at 190 nm in figures 6 and 7). Such an approach has no impact on the HOLD mission because the additional thrust is canceled by drag from the larger array.

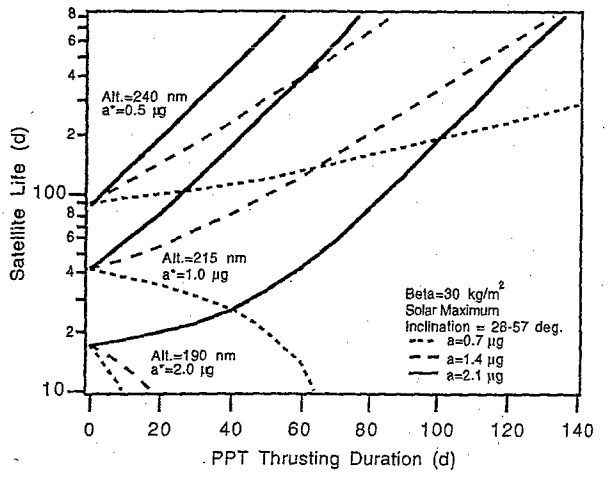

Figure 4: Satellite life extension using the Lift & Coast strategy (solar maximum, β=30 kg/m^2).

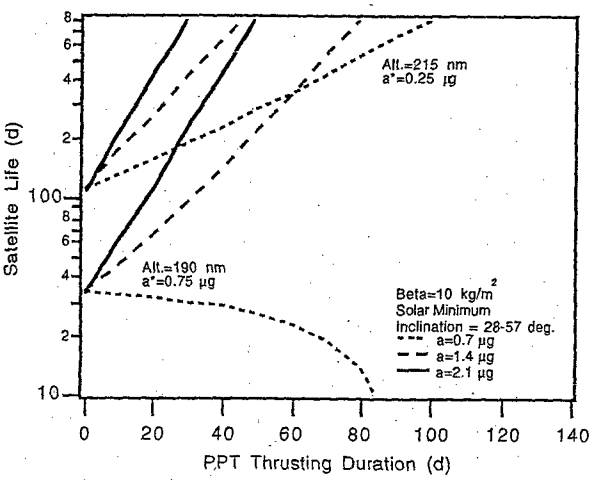

Figure 6: Satellite life extension using the Lift & Coast strategy (solar minimum, β=10 kg/m^2).

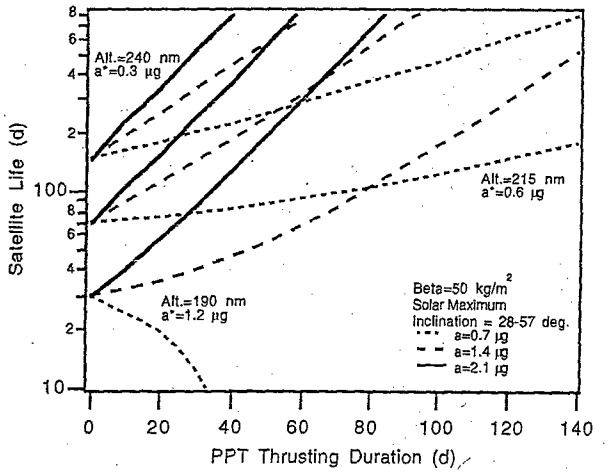

Figure 5: Satellite life extension using the Lift & Coast strategy (solar maximum, β=50 kg/m^2).

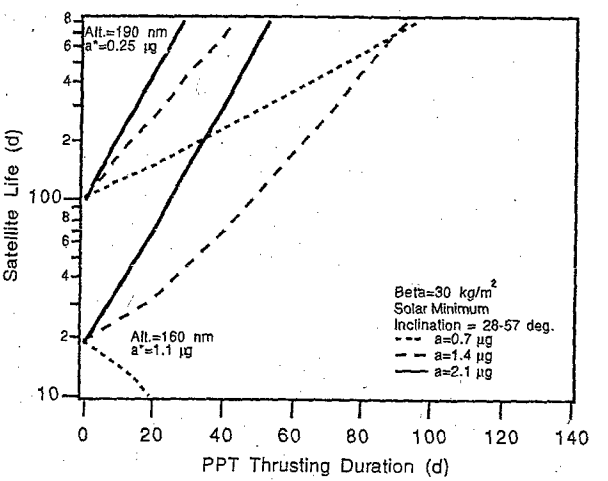

Figure 7: Satellite life extension using the Lift & Coast strategy (solar minimum, β=30 kg/m^2).

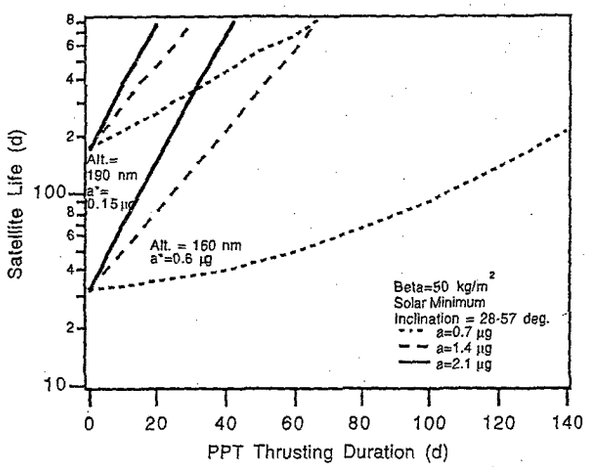

Figure 8: Satellite life extension using the Lift & Coast strategy (solar minimum, β=50 kg/m^2).

III.3 A Comparison of Hold and Lift & Coast

Hold and Lift & Coast represent the two basic strategies for extending satellite life; all other PPT thrusting schemes discussed in this paper represent compromises between these two. Hold, at its best, represents the ability to extend satellite life by operating the PPT throughout the mission at a very low power level. Lift & Coast does not require PPT operation during the payload's mission, but does require the payload to operate on standby power during the orbit raising maneuver after Shuttle deployment. In this section, the relative merits of each strategy are discussed in the context of a small satellite deployed from the Shuttle.

The principal advantage of Hold is the ability to use the PPT to extend satellite life *and* to operate the payload soon after Shuttle deployment. Unfortunately, there are many disadvantages associated with the Hold strategy when applied at Shuttle altitudes. First, the power and propellant mass requirements are generally too high to provide life extension to 1-2 years. Shown below in table 1 is the power and propellant mass requirements for both strategies for two representative cases: $a>>a^*$ and $a\sim a^*$.

a~a*	Lift & Coast	Hold
Transfer Time	128.5 d	0 d
Prop. Mass Fraction	0.016	0.034
Hold Power/Satellite Mass	0 W/kg	0.57 W/kg

Assumptions:
Init. Alt.=190 nm, solar maximum, β=50 kg/m^2, a=1.4 µg, a*=1.2 µg, life=1 year, I_{sp}=1000 sec, η=10%

a>>a*	Lift & Coast	Hold
Transfer Time	38.0 d	0 d
Prop. Mass Fraction	0.007	0.015
Hold Power/Satellite Mass	0 W/kg	0.14 W/kg

Assumptions:
Init. Alt.=240 nm, solar maximum, β=50 kg/m^2, a=2.1 µg, a*=0.3 µg, life=2 year, I_{sp}=1000 sec, η=10%

Table 1: A Comparison of Lift & Coast and Hold.

As shown in table 1, only when a^* is small (which is not satisfied in most regions of the trade space) does Hold start to make sense. For comparison, the PPT on the NOVA spacecraft was required to fire about once or twice per minute (a^* for NOVA was ~10^{-3} µg at solar maximum and ~10^{-4} µg at solar minimum[14,15]). Table 1 shows that for the above inputs and $a\sim a^*$, a 50 kg satellite requires 1.7 kg of propellant and 28.5 W of orbit-averaged power to extend the life to one year. This power level is very high for this class of satellite, and considering that the PPT dry mass can be as high as 8x the propellant mass, the PPT system mass could also be quite large.

A serious disadvantage of Hold results from the fact that power-limited propulsion for drag make-up is inherently unstable to multi-orbit time scale fluctuations in thermospheric density. Consider the scenario where a multi-day global rise in density reduces the satellite's altitude to the point where the PPT is unable to hold the satellite in orbit without more power. If at that point, the spacecraft is unable to provide more power to the PPT, the spacecraft will quickly fall out of orbit.

Potential sources of density fluctuations on this time scale include variations in solar UV flux and geomagnetic storms[26-29]. Density fluctuations from these phenomena are truly unpredictable in terms of when they occur, their duration and the magnitude of the density increase. The net effect of sub-orbit time scale density fluctuations, such as the motion of the satellite in and out of the diurnal bulge, should be small when averaged over an entire orbit, provided that the fluctuations are uncorrelated with satellite motion (see Appendix A and section III.5). Although the numbers shown in table 1 are calculated assuming $a=a^*$, some margin and/or peak power requirements must be implemented into the PPT/spacecraft design before such a strategy can be implemented. Considering this issue, the propellant mass fraction and hold power in table 1 should be taken as minimum values.

Lift & Coast is much less sensitive to density fluctuations because typically more power is available to lift the satellite, and because the satellite is at its lowest altitude for only a brief period of time at the beginning of the transfer. A design life of 1-2 years results in a high probability that a large multi-day density fluctuation will occur during the Hold mission. The average number of geomagnetic storms classified as *Severe* range from 0-5 per year depending on the time with respect to the solar cycle[28]. Geomagnetic storms classified as *Major* number about 5-20/year[28].

The primary advantage of Lift & Coast is that this strategy is feasible for most small satellite specific powers and at current SOA PPT performance levels. In addition, Lift & Coast eliminates the need to operate that PPT concurrently with the payload, thus enabling maximum power to the payload and simplified mission operations.

III.4 Lift & Hold and Related Strategies

There are various life extension strategies that can be used to provide a compromise between Lift & Coast and Hold. The use of these strategies will typically result in less power and propellant mass requirements than Hold, and a reduced transfer time compared to Lift & Coast. One strategy, which is designated Lift & Hold, is to use the full power available to the payload to boost the satellite's orbit up to a point where the PPT requires much less power and propellant to hold the satellite in orbit. Another strategy, Reduced-Power Lift, is to use the full payload power to boost the satellite up to a point where much less power is required to perform the remaining lift mission. For this strategy, the PPT is operated at full power to reduce the time that the drag force has to act on the satellite; when the drag force is no longer excessive, the PPT is powered-down, and the payload becomes operational for the reduced-power-lift phase of the maneuver and during the subsequent coast period. The final strategy examined, Lift/Coast/Reboost, requires the PPT to be used at full power to boost the satellite to a higher altitude; the PPT is then turned off, and the payload is allowed to operate in its nominal mode at full power until the satellite falls to the original altitude. At which point, the PPT is again used at full power to reboost the satellite to the same peak altitude. It certainly is not difficult to create a number of other combinations of the above life extension strategies.

Shown in figures 9 and 10 is a comparison of these strategies with Hold and Lift & Coast for two representative conditions: $a \sim a^*$ (fig. 9) and $a >> a^*$ (fig. 10). Plotted on the left scale is the specific power required, while the payload is operational, to perform the particular life extension strategy. On the right scale is the propellant mass fraction associated with providing 1 year (for $a \sim a^*$, fig. 9) or 2 years ($a >> a^*$, fig. 10) of on-orbit life. The horizontal scale is the full-power (payload on standby) PPT thrusting duration in days.

Starting with figure 9, it is seen that Hold (PPT full-power thrusting duration = 0 days) has the largest power and propellant mass requirements of all strategies, and Lift & Coast requires the longest duration of PPT full-power operation (128.5 d). Lift & Hold allows for a continuous distribution of power, mass fraction, and thrusting time between these two extremes. For instance, if the Lift & Coast PPT thrusting duration of 128.5 days is too long, Lift & Hold allows for it to be reduced considerably, although at the cost of propellant mass and power required to hold the satellite in orbit. For example, an 80 day transfer time increases the propellant mass fraction from 0.016 to 0.019 and hold power requirements from 0 to 0.19 W/kg. Although these values are high, they are much better than those corresponding to Hold (see table 1). When $a >> a^*$, significant reductions in trip time can be achieved with relatively small increases in propellant and power (see fig. 10). For instance, using Lift & Hold to reduce the transfer time to 10 days from 38 days requires a specific power level of 0.1 W/kg (plus margin to account for density disturbances) and only a slight increase in propellant fraction.

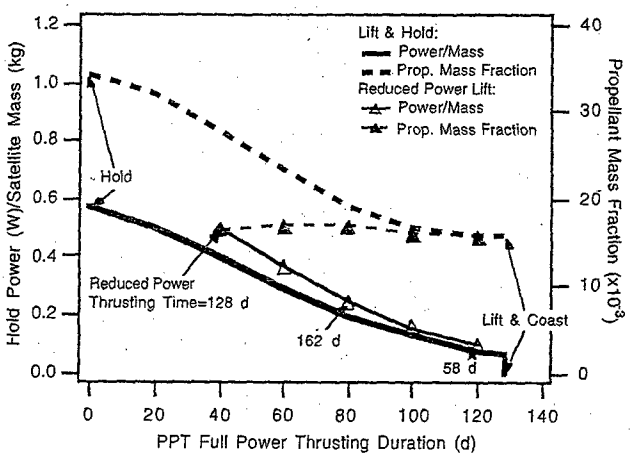

Figure 9: A comparison of life extension strategies for a representative $a \sim a^*$ case (init. alt.=190 nm, solar maximum, β=50 kg/m^2, a=1.4 μg, a^*=1.2 μg, I_{sp}=1000 sec, η=10%, 1 year design life).

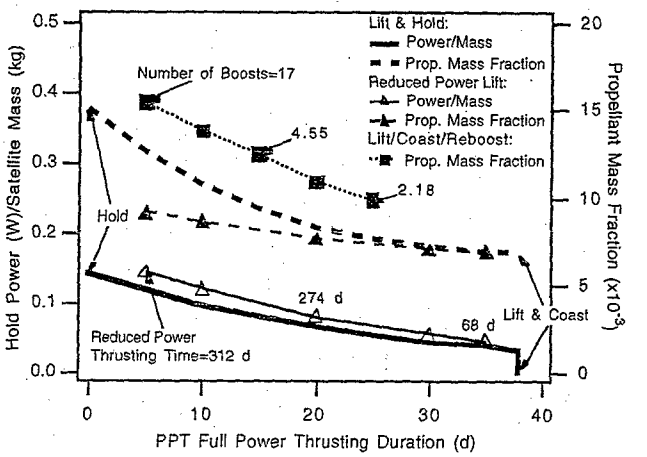

Figure 10: A comparison of life extension strategies for a representative $a >> a^*$ case (init. alt.=240 nm, solar maximum, β=50 kg/m^2, a=2.1 μg, a^*=0.3 μg, I_{sp}=1000 sec, η=10%, 2 year design life).

Reduced-Power Lift is another strategy which may prove useful. For figures 9 and 10, it was assumed that after full-power thrusting, the PPT power was reduced to the point where its orbit-averaged thrust was 25% greater than the drag force at that particular altitude. The PPT is then powered at this fixed level until it reaches an altitude where the decay time equals the desired life minus the reduced-power thrusting duration. As expected, Reduced-Power-Lift requires less propellant and more power than Lift & Hold. Also shown in figures 9 and 10 is the reduced-power thrusting durations for selected full-power transfer times.

Lift/Coast/Reboost was not plotted for the $a \sim a^*$ case because the transfer time is generally greater than the peak to original altitude decay time. Even for $a >> a^*$, short transfer times result in excessive propellant usage compared to the other strategies including Hold. By definition, there are no power requirements for this strategy when the payload is operational, and thus power is not plotted in figure 10.

Also shown in figure 10 is the number of boosts corresponding to each thrusting duration. For instance, instead of a single 38 day boost, a 2 year life can also be obtained by performing 17 5-day boosts at about 1-month intervals.

III.5 Drag Reduction Strategies

When designing a Shuttle-deployable satellite, it is certainly prudent to take advantage of any means to reduce the drag force, especially when $a \sim a^*$. Examining equation 1 suggests that there is not much that can be done to increase β without affecting a. Increasing spacecraft mass equally reduces a by the same factor which is undesirable because a has a greater effect on transfer time than β (see section III.2). For the same reason, reducing the spacecraft cross-sectional area (which is usually dominated by solar array area) is also undesirable due to its effect on spacecraft power. The final component of β, the drag coefficient, is relatively insensitive to spacecraft geometry at the orbital velocities corresponding to typical Shuttle altitudes.

One approach to increasing β is to align the solar arrays with the spacecraft velocity vector while the spacecraft is in the shade, thus reducing the orbit-averaged drag force without affecting power available to the PPT. Another approach is to align the arrays with the velocity vector as the spacecraft travels through the diurnal bulge (the region of maximum thermospheric mass density). A drawback of this latter strategy is the slight reduction of PPT power produced by performing such a maneuver. As expected, these strategies work best with satellites that have articulated arrays.

One method to quantify the benefits of such strategies is to consult equation A9 of Appendix A. The correlation term between the density and β, which was assumed to be small, is now non-negligible because the variation of density and solar array cross-sectional area is now correlated over an orbit. Using equation A9, it is easy to derive the following expression for β:

$$\frac{\beta}{\beta_{sp}} = \left[1 + \left(\frac{\overline{\tilde{\rho}/\tilde{\beta}}}{\overline{\rho}/\overline{\beta}}\right)\right]^{-1} \qquad (4)$$

where β_{sp} is the ballistic coefficient for a spacecraft that has solar arrays which are always pointing at the sun (even in the earth's shadow):

$$\beta_{sp} = \frac{m}{\overline{C_d}}\left[A_{body} + \frac{2}{\pi}A_{sa}\cos B\right]^{-1} \qquad (5)$$

where B is the sun-angle, i.e. the angle between the sun and orbital plane, A_{sa} is the solar array area, and A_{body} is the cross-sectional area of the spacecraft body, which is assumed constant. A spacecraft with sun-pointing arrays is typical and is used as a baseline for examining the benefits of these strategies. The evaluation of the correlation term is discussed in more detail in the Appendix; only the results will be discussed below.

Figure 11a shows a simplified geometry used to assess the benefits of performing this strategy. Generalizing the analysis is straight forward, and depends on mission specific parameters, such as time of the year, the orientation of the orbital plane with respect to the sun, and an accurate density model accounting for diurnal variation. It is assumed that the plane of the orbit is equatorial and the sun is at either Spring or Autumn equinox. It is further assumed that the density profile can be described by a cosine function, with a maximum associated with the diurnal bulge at 45 degrees[26,30,31] with respect to the earth-sun line, and minimum at 225 degrees:

$$\rho = \overline{\rho} + \rho_1 \cos(\theta - \pi/4) \qquad (6)$$

The first strategy examined is where the solar arrays are aligned with the velocity vector in the shade only. Figure 12 shows the extent at which β is increased by such a strategy assuming a range of A_{sa}/A_{body} and $\rho_1/\overline{\rho}$. Note that rising ρ_1 has the effect of reducing β, which at first thought may appear counterintuitive. This effect accounts for the density being lower than average in the earth's shadow, which reduces the impact of aligning the arrays in the shade. Although complicating flight operations, this strategy could also be used in the coast and/or hold portion of spacecraft flight operations.

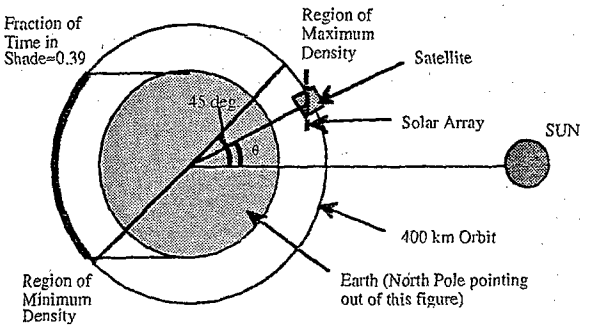

Figure 11a: Earth-sun-orbit geometry to illustrate the benefits of aligning the solar array with the spacecraft velocity vector to reduce the drag force.

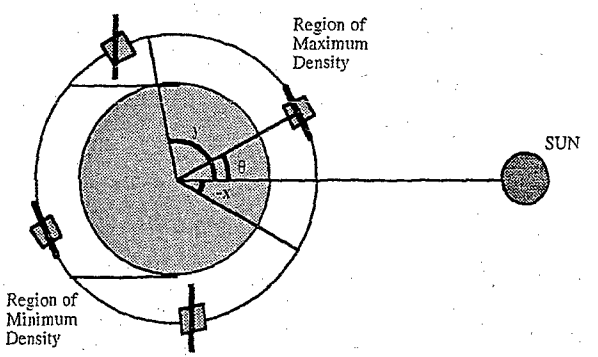

Figure 11b: Strategy for aligning the solar arrays with the spacecraft velocity vector in the earth's shadow and through the diurnal bulge.

Figure 13 illustrates the impact of using this strategy for $a \sim a^*$ and $a >> a^*$. Although the eclipse time and ρ_l vary with increased altitude, it was assumed that β was constant and 25% greater (see figure 12) than the nominal, sun-pointing value (β_{sp} =50 kg/m^2). This strategy significantly improves the PPTs ability to extend spacecraft life when the drag force is close to the PPT thrust (i.e. when $a \sim a^*$). When $a >> a^*$, aligning the arrays in the dark is much less effective, except when the strategy is also used during the coast phase. Use during the coast phase effectively reduces the transfer time because the PPT does not have to lift the satellite as high to achieve the same lifetime.

Figure 11b illustrates a more ambitious strategy to not only align the arrays with the velocity vector in the shade, but also for a short time through the diurnal bulge in an attempt to further reduce the drag force with limited impact on spacecraft power. As the spacecraft exits the shade, it points its arrays at the sun. At some point in the orbit, angle x, the arrays are rotated to align with the velocity vector with a corresponding reduction in power to the PPT (although insuring that the spacecraft bus power remains constant). The spacecraft then travels through the diurnal bulge with its arrays aligned with the velocity vector. At angle y, the arrays are repointed at the sun until entering the earth's shadow.

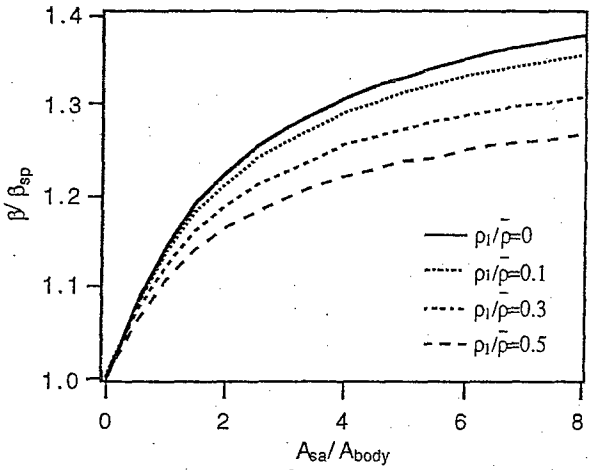

Figure 12: Increase in β by aligning solar arrays with spacecraft velocity vector in the earth's shadow for the case shown in figure 11a.

Figure 14 shows the effect of varying angle x and y for the situation shown in figure 11b, assuming that the ratio of bus power to payload power is 1, A_{sa}/A_{body}=10 and $\rho_l/\bar{\rho}$=0.5. Plotted is the ratio of the PPT orbit-averaged power to the nominal power level (arrays always sun-pointing) and the ratio of the orbit-averaged drag force to the nominal orbit-averaged drag force. Also shown is the difference between these two quantities; it is desired to maximize this difference to obtain the best performance when $a \sim a^*$. As seen in figure 14, there is indeed some benefit to aligning the arrays through the diurnal bulge, in addition to the shade region (note that aligning the arrays in the shade only corresponds to $x=y$). As the spacecraft altitude rises, the optimal x and y will very quickly shift to maximize power ($x=y$) as the PPT thrust begins to dominate the drag force. For this reason, performing such a maneuver will not be effective when $a >> a^*$. Of course, for each satellite program, further analysis is required to determine if such an operational scheme outweighs additional operations costs.

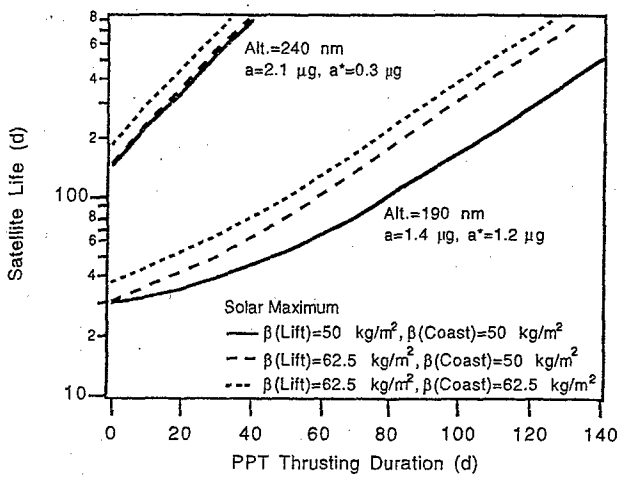

Figure 13: The effect of aligning the solar arrays with the spacecraft velocity vector in the earth's shadow assuming β/β_{sp}=1.25.

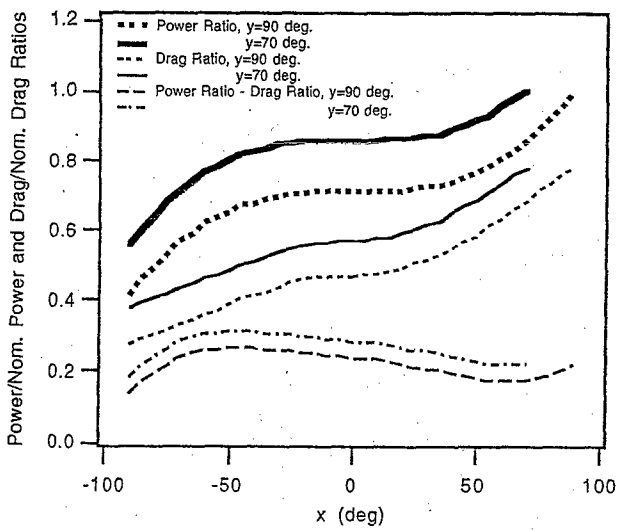

Figure 14: The effect of aligning the solar arrays with the spacecraft velocity vector in the earth's shadow and through the diurnal bulge, assuming the ratio of bus power to payload power is 1, A_{sa}/A_{body}=10, and $\rho_l/\bar{\rho}$=0.5.

III.6 Optimum Launch Windows

Recognizing that the small satellite operator may have limited influence on time of launch, there are seasons and times which are optimal for achieving maximum life-extension performance from the PPT. For example, the seasonal dependence of the globally-averaged thermospheric density has minimums at the Summer and Winter solstices, and maximums at the Spring and Autumn equinoxes. With the difference in density at Summer solstice and Spring equinox being 30-40% at Shuttle altitudes, it is certainly preferential to begin the orbit raising mission with such a benefit.

A further opportunity occurs when the orbit inclination is high, especially at the solstices, where it is possible to take advantage of all sun orbits with durations of over a week. Figure 15 shows the eclipse fraction as a function of the orbit right ascension of the ascending node, Ω, at the best-case situation of Summer solstice and an inclination of 57 degrees. For certain orbit plane orientations, those where the sun angle, B, is maximum, the eclipse fraction falls to zero. Starting a transfer in an all sun orbit allows for the thrust to be maximized during the portion of the transfer where drag is highest. An additional benefit of this particular sun-orbital plane configuration is that the solar array cross-sectional area in the direction of spacecraft motion is reduced considerably (see equation 5). The spacecraft cross-sectional area, with A_{body}=0.3 m^2 and A_{sa}=2.1 m^2, is shown in figure 15.

The initial Ω is determined by the time of day of the launch. The benefits of starting the orbit raising mission in an all sun orbit is shown in figure 16 (for $a \sim a^*$ and $a >> a^*$). These results were calculated with the model described in Appendix A with variable f_s, as determined by the orbital plane-earth-sun geometry accounting for Ω regression (see reference 32). Shown is a comparison of starting the orbit raising mission at Ω_0=200 degrees with respect to Spring equinox, and at Ω_0=135 degrees. Since Ω regresses at about -5 degrees per day (the sun position moves much slower), starting at 135 degrees can be considered worst case, while starting at 200 degrees allows for about 7-8 days of all sun light at the beginning of the transfer. The benefits of using this approach are generally small, except for when the thrusting durations are less than 10-20 days. Figure 16 shows that the difference between Ω_0=135 degrees and Ω_0=200 degrees is about 10 days of PPT operation. At the low inclinations, ~28 degrees, there exists no time during the year where the orbit is in all sunlight. This effect is also small for the high inclination orbits at the Spring and Autumn equinoxes.

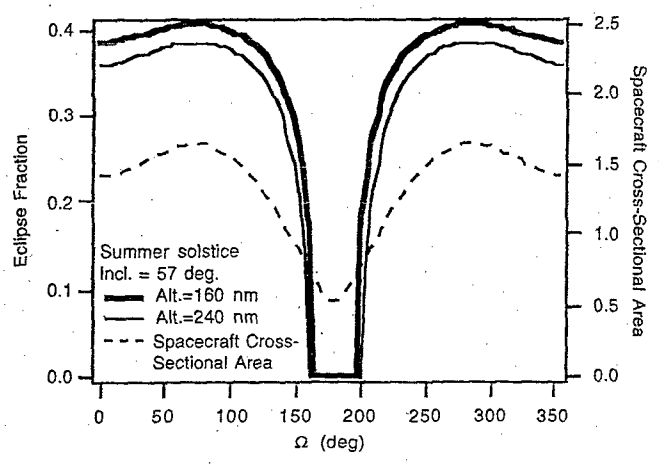

Figure 15: Eclipse fraction as a function of the right ascension of the ascending node at Summer solstice (A_{body}=0.3 m^2, A_{sa}=2.1 m^2).

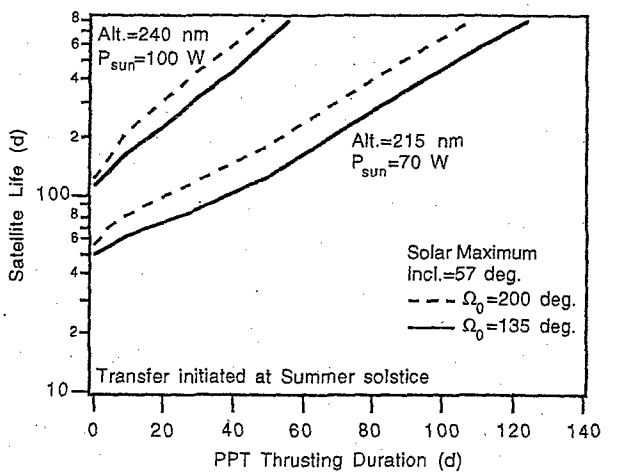

Figure 16: The effect of omega on satellite life (η=10%, I_{sp}=1000 sec, C_d=2, m=75 kg, A_{body}=0.2 m^2, A_{sa}=1.4 m^2).

IV. Conclusions

At typical Space Shuttle altitudes atmospheric drag is the dominant force limiting satellite on-orbit life (typically < 100 days). The pulsed plasma thruster (PPT) is ideally suited to extend the life of small satellites deployed from the Shuttle due to its low system mass and volume, high specific impulse, and inert solid propellant (teflon). The objective of this study was to identify and analyze life extension strategies for Space Shuttle-deployed small satellites using the pulsed plasma thruster. The generalized analysis presented in this paper should be independent of satellite, PPT performance and PPT life characteristics. The analysis has also been generalized for a wide range on on-orbit life requirements, although there was a focus on extending life to 1-2 years. This work also provides the basis for the design of next generation PPTs for this application, and resulted in the following conclusions:

1. There are many strategies, enough to fit most operational scenarios, for significantly extending small satellite on-orbit life. The most capable of these strategies, designated as Lift & Coast, requires the least amount of propellant, and should be capable of extending satellite life to 1-2 years with SOA PPT technology and with typical small satellite power to mass ratios. The Lift & Coast strategy consists of an initial orbit raising mission with the PPT utilizing all payload power. At the peak altitude of the transfer, which is determined from the satellite life requirement, the PPT is shut down for the remaining life of the satellite. The disadvantage of the Lift & Coast strategy is that the duration of the orbit raising maneuver can be as high as a few months.

2. The transfer time is extremely sensitive to the orbit-averaged power provided to the PPT (the more the better). When the trip time is too long, there are alternative strategies which may prove useful for extending satellite life (Lift & Hold, Lift/Coast/Reboost, Reduced-Power Lift) while reducing (but not eliminating) the duration of the full-power lift phase.

3. The strategy designated as Hold, which utilizes the PPT to maintain a satellite's altitude by supplying an orbit-averaged thrust to compensate for the drag force is impractical for providing a 1-2 year life at Shuttle-deployed altitudes. At typical small satellite power to mass ratios, the power and propellant requirements are too high to implement this strategy.

4. Other strategies to assist the mission of the PPT were also analyzed. The reduction of the orbit-averaged drag force, by aligning the solar arrays with the spacecraft velocity vector in the earth's shadow and through the diurnal bulge, had a significant effect on reducing the trip time in certain circumstances. Optimal launch windows which are beneficial for PPT operation were also identified. Starting the orbit raising maneuver near the June and December solstices is optimal due to the potential for all-sun orbits and lower than average global thermospheric densities.

References

1. Janson, S.W., "The On-Orbit Role of Electric Propulsion", AIAA Paper No. 93-2220, 1993.
2. Myers, R.M., et al., "Pulsed Plasma Thruster Technology for Small Satellite Missions", Proceedings of 9th AIAA/Utah State Univ. Conference on Small Satellites, Logan, UT, Sept. 1995.
3. Lorenz, R., "Small Satellites and Electric Propulsion - A Review", Aeronautical Journal, June/July 1991, pp. 204-213.
4. Sellers, J.J., "A Low-Cost Propulsion Option for Small Satellites", J. British Interplanetary Society, Vol. 48, pp. 129-138, 1994.
5. Myers, R.M., et al., "Small Satellite Propulsion Options", AIAA Paper No. 94-2997, 1994.
6. Sellers, J.J., et. al., "Investigation Into Low-Cost Propulsion Systems for Small Satellite Missions", Proceedings of 9th AIAA/Utah State Univ. Conference on Small Satellites, Logan, UT, Sept. 1995.
7. NASA Hitchhiker Customer Accomodations & Requirements Specifications, HHG-730-1503-07, Goddard Space Flight Center, Greenbelt, Maryland, 1994.
8. "Despite Delay, Contractor Eyes 1998 MightySat Launch", *Space News*, April 1-7, 1996, p. 15.
9. Vondra, R.J., Thomassen, K., Solbes, A., "Analysis of Solid Teflon Pulsed Plasma Thruster", J. Spacecraft & Rockets, Vol. 7, No. 12, pp. 1402-1406, 1970.
10. Guman, W.J. and Nathanson, D.M., "Pulsed Plasma Microthruster Propulsion System for Synchronous Orbit Satellite", J. Spacecraft & Rockets, Vol. 7, No. 4, pp. 409-415, 1970.
11. Braga-Illa, A., "Preliminary Report on the Orbital Operation of the Automatic Stationkeeping System of LES-6", AIAA Paper No. 69-934, 1969.
12. Guman, W.J. and Kowal, S.J., "Pulsed Plasma Propulsion System for TIP-II Satellite", Proceedings of the 1975 JANNAF Propulsion Meeting, Anaheim, CA, Sept. 1975, Vol. 1, pp. 443-457.
13. Kowal, S.J., "Post-Launch Results of the TIP Spacecraft Pulsed-Plasma Microthrusters", Proceedings of the 1980 JANNAF Propulsion Meeting, Monteray, CA, Mar. 1980, Vol. V, pp. 569-581.
14. Brill, Y., Eisner, A., Osborn, L., "The Flight Application of a Pulsed Plasma Microthruster; the NOVA Satellite", AIAA Paper No. 82-1956, 1982.
15. Ebert, W.L., Kowal, S.J., Sloan, R.F., "Operational Nova Spacecraft Teflon Pulsed Plasma Thruster System", AIAA Paper No. 89-2497, 1989.
16. Vondra, R.J. and Thomassen, K.I., "Flight Qualified Pulsed Plasma Thruster for Satellite Control", J. Spacecraft & Rockets, Vol. 11, No. 9, pp. 613-617, 1974.
17. Hirata, M. and Murakami, H., "Impulse Measurement of a Pulsed-Plasma Engine on Engineering Test Satellite-IV", J. Spacecraft & Rockets, Vol. 21, No. 6, pp. 553-556, 1984.
18. An, S.M., et al., "Space Flight Test of Electric Thruster System MDT-2A", J. Spacecraft & Rockets, Vol. 21, No. 6, pp. 593-594, 1984.
19. Vondra, R.J., "The MIT Lincoln Laboratory Pulsed Plasma Thruster", AIAA Paper No. 76-998, 1976.
20. Guman, W.J. and Williams, T.E., "Pulsed Plasma Microthruster for Synchronous Meteorological Satellite (SMS)", AIAA Paper No. 73-1066, 1973.
21. Tilley, D.L., et al., "Advanced Pulsed Plasma Thruster Demonstration on MightySat Flight II.1", Abstract submitted to the 10th AIAA/Utah State Univ. Conference on Small Satellites, Logan, UT, Sept. 1996.
22. Isakowitz, S.J., "Space Launch Systems", 2nd Ed., AIAA Press, Washington DC, 1991.
23. Proceedings of 9th AIAA/Utah State Univ. Conference on Small Satellites, Logan, UT, Sept. 1995. (See also past years proceedings).
24. "Solar Activity Inputs for Upper Atmospheric Models Used in Programs to Estimate Spacecraft Orbital Lifetime", Monthly Memorandum from the Electromagnetics and Aerospace Environments Branch, NASA Marshall Space Flight Center, AL.
25. Zondervan, K.P., et al., "Operational Requirements for Cost Effective Payload Delivery with Solar Electric Propulsion", 23rd International Electric Propulsion Conference, IEPC Paper No. 93-203, Seattle, WA, 1993.
26. Hedin, A.E., "MSIS-86 Thermospheric Model", J. Geophys. Res., Vol. 92, No. A5, pp. 4649-4662, 1987.
27. Hedin, A.E. and Mayr, H.G., "Solar EUV Induced Variations in the Thermosphere", J. Geophys. Res., Vol. 92, No. D1, pp. 869-875, 1987.
28. Walterscheid, R.L., "Solar Cycle Effects on the Upper Atmosphere: Implications for Satellite Drag", J. Spacecraft & Rockets, Vol. 26, pp. 439-444, 1989.
29. Withbroe, G.L., "Solar Activity Cycle: History and Predictions", J. Spacecraft & Rockets, Vol. 26, pp. 394-402, 1989.
30. Marcos, F.A., et al., "Operational Satellite Drag Model Standards", AIAA Paper No. 95-0551, 1995.
31. Hedin, A.E., "A Revised Thermospheric Model Based on Mass Spectrometer and Incoherent Scatter Data: MSIS-83", J. Geophys. Res., Vol. 88, No. A12, pp. 10170-10188, 1983.
32. Larson, W.J. and Wertz, J.R., editors, *Space Mission Analysis and Design*, 2nd Edition, Microcosm, Inc. and Kluwer Academic Publishers, 1992.

33. Dickey, M.R., et al., "Development of The Electric Vehicle Analyzer", AL-TR-90-006, June 1990.
34. Bate, R.B., Mueller, D.D., White, J.E., *Fundamentals of Astrodynamics*, Dover Publications, Inc., NY, NY, 1971.
35. Marcos, F.A., et al., "Operational Satellite Drag Model Standards", AIAA Paper No. 95-0551, 1995.
36. Hedin, A.E., Spencer, N.W., Killeen, T.L., "Empirical Global Model of Upper Thermosphere Winds Based on Atmosphere and Dynamics Explorer Satellite Data", J. Geophys. Res., Vol. 93, No. A9, pp. 9959-9978, 1988.
37) Marcos, F.A., "Accuracy of Atmospheric Drag Models at Low Satellite Altitudes", Adv. Space Res., Vol. 10, pp.417-422, 1990.

Nomenclature

$a(t)$	Instantaneous spacecraft acceleration due to PPT thrust
a, $\bar{a}$	Orbit-averaged spacecraft acceleration due to PPT thrust
a^*	Value of a required for orbit-averaged PPT thrust to equal the drag force at the Shuttle-deployed altitude
$\tilde{a}$	Time varying component of $\tilde{a}$ = a(t)-a (see Appendix A)
$A(t)$	Instantaneous satellite cross-sectional area
$\bar{A}$	Orbit-averaged satellite cross-sectional area
A_{body}	Orbit-averaged satellite body cross-sectional area
Ap	Geomagnetic activity parameter
A_{sa}	Total solar array area
B	Angle between sun and the orbital plane
C_d	Instantenous satellite drag coefficient
$\bar{C}_d$	Orbit-averaged satellite drag coefficient
e	Orbit eccentricity
f_s	Fraction of the orbit in sunlight
$F_{10.7}$	Solar radiative flux at 10.7 cm
F_D	Instantaneous drag force
g	Gravitational acceleration at the earth's surface
g_l	Gravitational acceleration at the local altitude
i	Orbit inclination
I_{sp}	PPT specific impulse
m	Spacecraft mass
m_i	Spacecraft mass at orbit i
m_0	Spacecraft mass at the start of the thrusting maneuver
$\dot{m}$	PPT average mass flow rate
m_{prop}	Propellant mass expelled by PPT
P	Average power input to PPT
r	Orbit radius
$\bar{r}$	Orbit-averaged radius
$\tilde{r}$	Time-varying radius $\tilde{r} = r - \bar{r}$ (see Appendix A)
r_0	Initial orbit radius
r_i	Orbit radius after i orbits
R_e	Earth radius
t	Time
t_0	Time at start of thrusting maneuver
t_i	Time after i orbits
t_p	Orbital period
t_{pi}	Orbital period during orbit i
T	"Instantaneous" thrust on a time scale much greater than the PPT inverse pulse frequency
T_e	Earth rotational period
$\bar{T}_{s,d}$	Time-averaged PPT thrust in sunlight (s) and in shadow (d)
V	Spacecraft geocentric velocity
V_1	See equation A9
$\vec{V}_e$	Rotational velocity of the earth at the equator
$\vec{V}_w$	Thermospheric wind velocity
$\tilde{V}_w$	$= \vec{V}_w(t) \cdot \hat{V}(t)$
$\hat{V}$	Unit vector in the direction of satellite motion
x, y	See figure 11b
$\beta(t)$	Instantaneous satellite ballistic coefficient ($\beta(t) \equiv m/C_d A$)
β, $\bar{\beta}$	Orbit-averaged satellite ballistic coefficient
$\tilde{\beta}$	Time-varying component of β (see Appendix A)
β_{sp}	Orbit-averaged ballistic coefficient for a satellite with sun-pointing arrays
η	PPT system efficiency
θ	See figure 11b
μ	Earth's gravitational parameter
ρ	Instantaneous thermospheric mass density
$\bar{\rho}$	Globally-averaged thermospheric mass density
$\tilde{\rho}$	Time-varying component of the denisty: $\tilde{\rho} \equiv \rho - \bar{\rho}$
ρ_1	Amplitude of time varying component of ρ (see equation 5)
Ω	Right ascension of the accending node
Ω_0	Initial right ascension of the accending node at the start of the orbit raising maneuver

Appendix A

In this appendix, the numerical routine used in this analysis is derived including the identification of all critical assumptions. The routine is based on that of the Electric Vehicle Analyzer code[33] originally developed at the Phillips Laboratory, with many modifications. As will be shown below, the routine is simple to implement and is quite accurate when all assumptions are satisfied (which is usually the case when modeling electric propulsion orbit raising and de-orbit missions).

First, it is assumed that the earth's gravitational force, the PPT thrust, and atmospheric drag are the dominant orbit-averaged forces on the spacecraft, and that the net effect of all other perturbation forces (e.g. radiation pressure, earth oblateness effects, lift forces, moon and sun gravitational forces) are negligible when averaged over an orbit. The inclusion of the dominant earth oblateness effect, the regression of the right ascension of the ascending node (Ω), is discussed in more detail in section III.6. Assuming an initial near-circular orbit ($e<<1$, where e is the orbit eccentricity), and that the orbit remains near-circular throughout the maneuver (which is typically the case), the following expressions for Newton's 2nd law are valid[34]:

$$T - F_D = m(r\ddot{\theta} + 2\dot{r}\dot{\theta}) \qquad \text{(A1)}$$

$$\frac{-\mu m}{r^2} = m(\ddot{r} - r\dot{\theta}^2) \qquad \text{(A2)}$$

where T and F_D are the thrust and drag forces, m is the spacecraft mass, μ is the product of the universal gravitational constant and the mass of the earth, and r, θ are the polar coordinates for motion in a plane. Assuming $\ddot{r} << r\dot{\theta}^2$, the following equation for the change in orbit radius with respect to time can be derived from equations A1 and A2:

$$\frac{dr}{dt} = \frac{2}{m}\sqrt{\frac{r^3}{\mu}}(T - F_D) \qquad \text{(A3)}$$

To check the last assumption, it can be shown that:

$$\frac{\ddot{r}}{r\dot{\theta}^2} \sim \left[\frac{(T-F_D)}{m}\frac{r^2}{\mu}\right]^2 = \left[\frac{(T-F_D)}{mg_l}\right]^2$$

which is easily satisfied for low-thrust orbit raising maneuvers. Using the MightySat mission as an example, T-F_D~2 mN, m~100 kg, g_l=8.7 m/s^2 for a 400 km orbit gives $\ddot{r} / r\dot{\theta}^2 \sim 10^{-12}$.

The instantaneous drag force on the satellite is determined from the following equation[35]:

$$F_D = \frac{1}{2}\rho C_d A\left[V - \vec{V}_e \cdot \hat{V} - \vec{V}_w \cdot \hat{V}\right]^2 \qquad \text{(A4)}$$

where ρ is the thermospheric mass density, C_d is the satellite drag coefficient, $\hat{V}$ is a unit vector in the direction of the satellite velocity vector, A is the satellite projected area in the direction of $\hat{V}$, V is the geocentric velocity of the spacecraft, and V_e and V_w are the earth's rotational velocity at nadir and the local thermospheric wind velocity respectively. Most of the parameters in equation A4 vary throughout the duration of one orbit.

The earth's rotational velocity term accounts for the fact that the thermosphere rotates with the earth, thus reducing drag for direct orbits and increasing drag for retrograde orbits. The component of the rotational velocity in the direction of satellite motion is constant throughout an orbit, with a value given by the following expression:

$$\vec{V}_e \cdot \hat{V} = \pm\frac{2\pi R_e}{T_e}\cos i = (0.46 km/\sec)\cos i \qquad \text{(A5)}$$

where R_e and T_e are the earth's mean radius and rotation period respectively, and i is the orbit inclination, and the $\pm$ reflects the distinction between direct and retrograde orbits.

Substituting eq. A5 and A4 into eq. A3, and using $V^2=\mu/r$ for a circular orbit, results in the following differential equation for determining $r(t)$:

$$\frac{dr}{dt} = 2\sqrt{\frac{r(t)^3}{\mu}}\left\{a(t) - \frac{\rho(r,t)}{2\beta(t)}\left[\sqrt{\frac{\mu}{r(t)}} \pm \frac{2\pi R_e}{T_e}\cos i - V_w(t)\cdot\hat{V}(t)\right]^2\right\} \qquad \text{(A6)}$$

where:

$$a(t) = \frac{T(t)}{m(t)} \qquad \text{and} \qquad \beta(t) = \frac{m(t)}{C_d(t)A(t)}$$

$a(t)$ is the instantaneous spacecraft acceleration with only the electric thruster imparting momentum to the vehicle, and $\beta(t)$ is the instantaneous ballistic coefficient. The following differential equation has no closed-form solution. For this reason, the approach is taken to calculate the average value of the altitude rate of change over one orbit. By doing this, the radius of the orbit at any time can be determined from the following relations:

$$r_i = r_0 + \sum_{j=0}^{i-1} t_{pj}\left(\overline{\frac{dr}{dt}}\right)_{r=r_j} \qquad \text{(A7)}$$

$$t_i = t_0 + \sum_{j=0}^{i-1} t_{pj} \qquad \text{(A8)}$$

where: $$t_{pj} = 2\pi\sqrt{\frac{r_j^3}{\mu}}$$

where r_i and t_i denote the orbit radius and time after orbit i, and r_0 and t_0 represent the initial orbit radius and starting time of the orbit raising maneuver. Generally, this scheme provides sufficient spatial and temporal resolution because a typical orbit raising maneuver involves on the order of 100s or 1000s of orbits, and because r_i does not change much from orbit to orbit. Second order terms in equation A7 are neglected, and are on the order of $(T\text{-}F_D)/mg_l << 1$. The orbit period at $r=r_j$ is denoted by t_{pj}; although t_{pj} changes slightly during one orbit, the effect is second order with a correction term also on the order of $(T\text{-}F_D)/mg_l << 1$.

To facilitate the calculation of the orbit-averaged dr/dt, the following relations where substituted into eq. A6:

$$r(t) = \bar{r} + \tilde{r}(t)$$
$$a(t) = \bar{a} + \tilde{a}(t)$$
$$\rho(r,t) = \bar{\rho}(r) + \tilde{\rho}(t)$$
$$\beta(t) = \bar{\beta} + \tilde{\beta}(t)$$
$$V_w(t)\cdot\hat{V}(t) = \tilde{V}_w(t)$$

The bar over the above parameters denotes the orbit-averaged value, and the tilde represents a time-varying component, where $\overline{\tilde{r}(t)} = \overline{\tilde{a}(t)} = \overline{\tilde{\rho}(t)} = \overline{\tilde{\beta}(t)} = \overline{\tilde{V}_w(t)} = 0$ and the following relative magnitudes hold:

$$\frac{\tilde{r}(t)}{\bar{r}} \sim e << 1 \qquad \tilde{\rho}(t) \sim \bar{\rho}(r) \qquad \tilde{V}_w << V$$

$$\tilde{a}(t) \sim \bar{a} \equiv \frac{\bar{T}}{m_0} \qquad \tilde{\beta} \le \bar{\beta} \equiv \frac{m_0}{C_d A}$$

where m_0 is the initial spacecraft mass. Substituting the above relations into equation A7, and assuming that $\bar{r} \cong r_i$ and $m_i >> \dot{m}t_{pi}$ (where $\dot{m}$ is the time-averaged mass flow rate of the PPT), the following expression can be derived:

$$\left(\frac{\overline{dr}}{dt}\right)_{r=r_i} = \frac{1}{\pi} t_{pi} \frac{m_0}{m_i} \bullet \left(\bar{a} - \frac{\overline{\rho}(r_i) V_1^2}{2\bar{\beta}} \left\{ 1 + \frac{\overline{\tilde{\rho}/\tilde{\beta}}}{\overline{\rho}(r_i)/\bar{\beta}} - \frac{2\overline{\tilde{V}_w/\tilde{\beta}}}{V_1/\bar{\beta}} - \frac{\overline{\tilde{\rho}\tilde{V}_w}}{\overline{\rho}(r_i)V_1} \right\} \right) \quad \text{(A9)}$$

where: $$V_1 = \sqrt{\frac{\mu}{r_i}} \pm \frac{2\pi R_e}{T_e} \cos i$$

and all higher order terms were neglected. The magnitude of the three cross-terms are evaluated as follows. The term $(\overline{\tilde{\rho}/\tilde{\beta}}/\overline{\rho}/\bar{\beta})$~0 because the variation in atmospheric density throughout an orbit is essentially uncorrelated with β when the solar arrays are sun-tracking. This term is non-negligible when a life extension strategy such as aligning the arrays with the velocity vector in the earth's shadow is implemented (see section III.5). The terms $(\overline{\tilde{V}_w/\tilde{\beta}}/V_1/\bar{\beta})$ and $(\overline{\tilde{\rho}\tilde{V}_w}/\overline{\rho}V_1)$ are also assumed to be negligible because usually $V_w << V$[36]. The wind velocity is typically on the order of 100-200 m/sec, although it can be as high as 1 km/sec during geomagnetic storms[35-37]. Neglecting these latter two terms may invalidate the numerical scheme when modeling thrusting maneuvers during extended periods of geomagnetic activity.

Substituting equation A9 into equation A7, and neglecting the cross-terms in equation A9 results in following expression for the orbit radius:

$$r_i = r_0 + \frac{1}{\pi} \sum_{j=0}^{i-1} t_{pj}^2 \frac{m_0}{m_j} \left\{ \bar{a} - \frac{\overline{\rho}(r_j)}{2\bar{\beta}} \left[\sqrt{\frac{\mu}{r_j}} \pm \frac{2\pi R_e}{T_e} \cos i \right]^2 \right\} \quad \text{(A10)}$$

The mass of the satellite, and thus the propellant mass used, can be determined from the following relation:

$$m_i = m_0 \left[1 - \frac{\bar{a}}{I_{sp} g} t_i \right] \quad \text{(A11)}$$

Given electric thruster and satellite characteristics $(\bar{a}, \bar{\beta})$, equations A8, A10, and A11 are the three basic equations used to determine the time history of the orbit radius and satellite mass.

Application to Satellite Maneuvering Using the PPT

Using the PPT to extend the life of small satellites deployed from the Space Shuttle allows for a few more simplifying assumptions. First, although the PPT uses 5-10 μsec duration impulse bits to provide thrust, it is the time-averaged thrust that is used in this analysis. This approach is valid if the orbit raising mission is much greater than the inverse pulse rate. Also, a PPT generally does not use much propellant over an entire mission; mass fractions are typically >99% for the life extension mission. For this reason, it is assumed that $\bar{a}$ and $\bar{\beta}$ do not vary throughout the mission. With these assumptions, and eliminating the bars above $\bar{a}$ and $\bar{\beta}$, equation A10 and A11 become:

$$r_i = r_0 + \frac{1}{\pi} \sum_{j=0}^{i-1} t_{pj}^2 \left\{ a - \frac{\overline{\rho}(r_j)}{2\beta} \left[\sqrt{\frac{\mu}{r_j}} - \frac{2\pi R_e}{T_e} \cos i \right]^2 \right\} \quad \text{(A12)}$$

$$\frac{m_{prop}}{m_0} = \frac{a}{I_{sp} g} (t_i - t_0) << 1 \quad \text{(A13)}$$

Power requirements are determined from the following relation:

$$\frac{P}{m_0} = a \frac{I_{sp} g}{2\eta} \quad \text{(A14)}$$

In all of the analysis performed in this study, the relation shown in A13 was verified to be valid. This allows for the expression for $r(t)$ to be independent of the mass of the spacecraft, and thus independent of the PPT specific impulse. In addition, for all of the analysis performed, it was assumed that the Shuttle orbit was direct with an inclination of 44.4 degrees (which corresponds to the average value of cos i when i is between 28 and 57 degrees). This assumption is very good considering that the earth's rotational velocity has a small effect on the drag, and allows for the elimination of i from the trade space. With these assumptions it is seen that $r(t)$ depends on four parameters: a, β, r_0, and $\rho(r)$ (which can be characterized by $F_{10.7}$).

For the Hold mission, the value of a required to maintain the spacecraft orbit is given by the following expression:

$$a^* = \frac{\rho(r_0)}{2\beta} \left[\sqrt{\frac{\mu}{r_0}} - \frac{2\pi R_e}{T_e} \cos i \right]^2 \quad \text{(A15)}$$

where a^* corresponds to the value of a required to compensate exactly for the drag force at the Shuttle-deployed altitude. The propellant mass and power required for Hold are determined from equations A13 and A14.

Thermospheric Density Model

The thermospheric density model used in this study was the MSIS-86 model[26]. The terms in the thermospheric model required for this analysis include the time-independent terms and those accounting for solar activity (as characterized by $F_{10.7}$). These terms provide the density as a function of $F_{10.7}$ and latitude. To obtain the globally-averaged density, the density as a function of latitude was then averaged. All other terms (diurnal, semidiurnal, longitudinal, etc.) are negligible when averaged over a single orbit, except the for those accounting for geomagnetic activity. Geomagnetic activity was not accounted for in this study (Ap=4). The MSIS-86 model is state-of-the-art, and has compared very well with in-flight measurements (~10%)[37].